

chromatin entry site activities of TREs are functionally separated. Cumulatively, our results support a model in which RNAs transcribed from the TREs of *Ubx* are retained at TREs through DNA-RNA interactions and provide a RNA scaffold that is bound by Ash1.

References and Notes

- R. Jaenisch, A. Bird, *Nat. Genet.* **33** (suppl.), 245 (2003).
- B. M. Turner, *Cell* **111**, 285 (2002).
- V. Orlando, *Cell* **112**, 599 (2003).
- L. Ringrose, R. Paro, *Annu. Rev. Genet.* **38**, 413 (2004).
- A. Breiling, V. Orlando, *Nat. Struct. Biol.* **9**, 894 (2002).
- P. B. Becker, W. Horz, *Annu. Rev. Biochem.* **71**, 247 (2002).
- T. Jenuwein, C. D. Allis, *Science* **293**, 1074 (2001).
- R. Cao, Y. Zhang, *Curr. Opin. Genet. Dev.* **2**, 155 (2004).
- C. Beisel, A. Imhof, J. Greene, E. Kremmer, F. Sauer, *Nature* **419**, 857 (2002).
- N. Tripoulas, D. Lajeunesse, J. Gildea, A. Shearn, *Genetics* **143**, 913 (1996).
- D. Lajeunesse, A. Shearn, *Mech. Dev.* **53**, 123 (1995).
- S. Schmitt, M. Prestel, R. Paro, *Genes Dev.* **19**, 697 (2005).
- G. Rank, M. Prestel, R. Paro, *Mol. Cell. Biol.* **22**, 8026 (2002).
- E. Bae, V. C. Calhoun, M. Levine, E. B. Lewis, R. A. Drewell, *Proc. Natl. Acad. Sci. U S A.* **99**, 16847 (2002).
- H. D. Lipshitz, D. A. Peattie, D. S. Hogness, *Genes Dev.* **1**, 307 (1987).
- J. Dejardin *et al.*, *Nature* **434**, 533 (2005).
- T. Rozovskaia *et al.*, *Mol. Cell. Biol.* **19**, 6441 (1999).
- C. H. Martin *et al.*, *Proc. Natl. Acad. Sci. USA* **92**, 8398 (1995).
- See supporting material on Science Online.
- A. Akhtar, *Curr. Opin. Genet. Dev.* **13**, 161 (2003).
- A. Wutz, *Bioessays* **25**, 434 (2003).
- E. Heard, *Curr. Opin. Cell Biol.* **16**, 247 (2004).
- M. A. Matzke, J. A. Birchler, *Nat. Rev. Genet.* **6**, 24 (2005).
- W. A. Krajewski, T. Nakamura, A. Mazo, E. Canaani, *Mol. Cell. Biol.* **25**, 1891 (2005).
- S. R. Albright, R. Tjian, *Gene* **242**, 1 (2000).
- T. Maille, S. Kwoczyński, R. J. Katzenberger, D. A. Wassarman, F. Sauer, *Science* **304**, 1010 (2004).
- H. Kawasaki, K. Taira, *Curr. Opin. Mol. Ther.* **7**, 125 (2005).
- C. B. Phelps, A. H. Brand, *Methods* **14**, 367 (1998).
- E. J. Sontheimer, *Nat. Rev. Mol. Cell Biol.* **6**, 127 (2005).
- V. Schranke, R. Allshire, *Curr. Opin. Gen. Dev.* **14**, 174 (2004).
- A. Verdel *et al.*, *Science* **303**, 672 (2004); published online 2 January 2004 (10.1126/science.1093686).
- M. J. O'Neill, *Hum. Mol. Genet.* **14** Spec No 1:R113 (2004).
- S. W.-L. Chan *et al.*, *Science* **303**, 1336 (2004).
- S. I. Grewal, J. C. Rice, *Curr. Opin. Cell Biol.* **16**, 230 (2004).
- M. Christmann, M. T. Tomacic, W. P. Roos, B. Kaina, *Toxicology* **193**, 3 (2003).
- Y. Chen, G. Varani, *FEBS J.* **272**, 2088 (2005).
- F. H. Allain, P. W. Howe, D. Neuhau, G. Varani, *EMBO J.* **16**, 5764 (1997).
- V. H. Meller, B. P. Rattner, *EMBO J.* **21**, 1084 (2002).
- We thank J. A. Diaz-Pendon, E. Poon, and M. Rubalcava for support with RACE, tissue culture, and disc preparation, and members of the Sauer lab for helpful comments that improved the manuscript. F.S. thanks S. Angle for support. Supported by Deutsche Forschungsgemeinschaft (DFG) research fellowship SA1010/1-1 (T.S.-E.), a DFG/Transregio-5 grant (E.K.), and NIH grant GM073776 and VolkswagenStiftung grant I/79-725 (F.S.).

Supporting Online Material

www.sciencemag.org/cgi/content/full/311/5764/1118/DC1

Materials and Methods

Figs. S1 to S16

Tables S1 to S3

References

20 July 2005; accepted 23 January 2006

10.1126/science.1117705

A Swimming Mammaliaform from the Middle Jurassic and Ecomorphological Diversification of Early Mammals

Qiang Ji,^{1,3} Zhe-Xi Luo,^{2,1*} Chong-Xi Yuan,³ Alan R. Tabrum²

A docodontan mammaliaform from the Middle Jurassic of China possesses swimming and burrowing skeletal adaptations and some dental features for aquatic feeding. It is the most primitive taxon in the mammalian lineage known to have fur and has a broad, flattened, partly scaly tail analogous to that of modern beavers. We infer that docodontans were semiaquatic, convergent to the modern platypus and many Cenozoic placentals. This fossil demonstrates that some mammaliaforms, or proximal relatives to modern mammals, developed diverse locomotory and feeding adaptations and were ecomorphologically different from the majority of generalized small terrestrial Mesozoic mammalian insectivores.

The Middle Jurassic mammalian diversification gave rise to several emergent clades: basal eutriconodontans, amphitheriid cladotherians, the basal mammalian lineage of shuotheriids, and basal australosphenidans (1–5). These new clades of crown Mammalia coexisted with several mammaliaform lineages (the proximal relatives to modern mammals) (1, 6–8). Docodontans are a Mesozoic mammaliaform lineage that have specialized molars for omnivorous feeding;

several taxa are known from the Middle Jurassic (1, 9–13). Here, we report on a large docodontan mammaliaform that has some dental features for feeding on aquatic invertebrates and small vertebrates, plus specialized skeletal and soft-tissue features for swimming and burrowing.

Description and comparison. *Castorocauda lutrasimilis*, gen. et sp. nov. (14), is from the Middle Jurassic Jiulongshan Formation, dated to be approximately 164 million years ago (15–17). The fauna includes pterosaurs (17, 18), a coelurosaurian dinosaur (19), lissamphibians (20), abundant fossil insects (21), and the conchostracan *Euestheria* (22). The holotype of *C. lutrasimilis* (Fig. 1) is represented by a partial skeleton (preserved rostrum-tail length

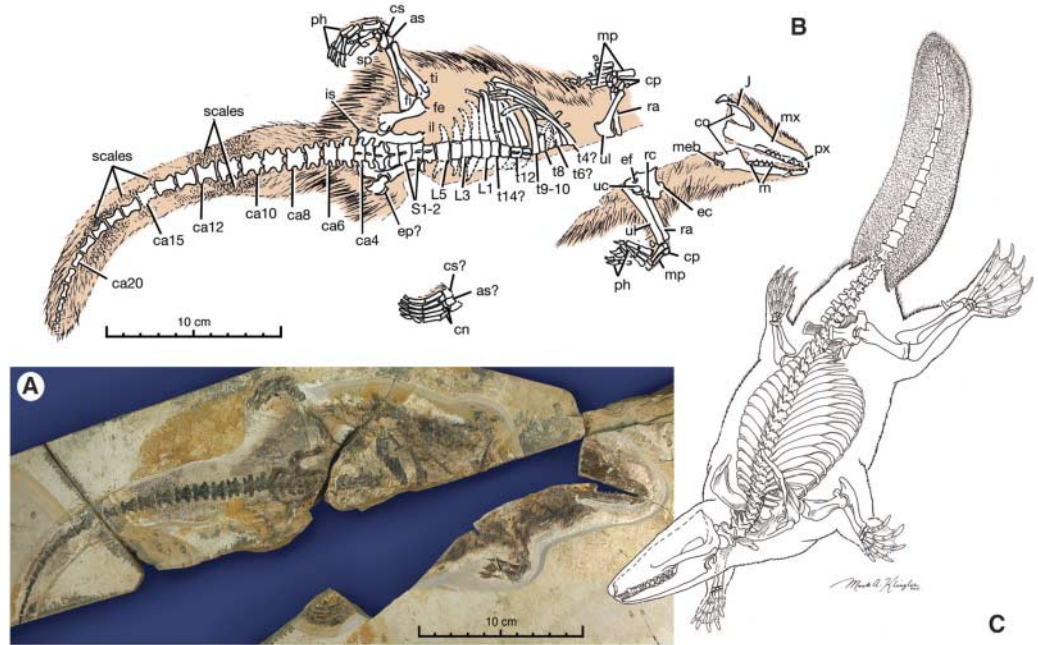
≥425 mm) with incomplete cranium (preserved length ≥60 mm) but well-preserved mandibles and lower dentition (incisors 4, canine 1, premolars 5, molars 6). Lower molars 3 to 6 have the diagnostic characteristics of docodontans (Fig. 2): anteriorly placed and enlarged lingual cusp g, triangulated crests formed by cusps a-c and a-g, and two partially enclosed basins formed respectively by cusps a, b, and g, and by cusps a, c, and d (9–12). As in all docodontans, the molars were capable of both shearing by the triangulated crests and grinding between the anterior (“pseudotalonid”) basin and the transversely widened upper molars (9–12). *Castorocauda* is distinctive from other docodontans in having mediolaterally compressed crowns of molars 1 and 2, each with five cusps in straight alignment (23, 24); primary cusp a and posterior cusps c and d are slightly recurved (Fig. 2). These “triconodont-like” anterior molars are plesiomorphic for mammaliaforms (6–8) but nonetheless distinctive among docodontans. They are convergent to those of placental mesonychians and Eocene whales (25). This type of molar with recurved cusps in alignment is hypothesized to be a specialization for feeding on fish and aquatic invertebrates by functional analogy to the teeth of modern pinniped carnivores such as seals.

Castorocauda is preserved with intact middle ear bones (Fig. 2) on the mandible, including the articular (malleus), the surangular, and the angular (ectotympanic). The middle ear bones in anatomical association with the mandible corroborate a previous interpretation of the middle ear in docodontans (26). A concavity on the

¹Department of Earth Science, Nanjing University, Nanjing 200017, China. ²Carnegie Museum of Natural History, Pittsburgh, PA 15213, USA. ³Chinese Academy of Geological Sciences, Beijing 100037, China.

*To whom correspondence should be addressed. E-mail: LuoZ@CarnegieMNH.org

Fig. 1. Holotype of *Castorocauda lutrasimilis* [Jinzhou Museum of Paleontology (JZMP) 04-117]. **(A)** Photograph of the holotype. **(B)** Osteological structures and preserved soft-tissue features. **(C)** Reconstruction of *Castorocauda lutrasimilis* as a swimming and burrowing mammaliaform. Abbreviations: as, astragalus; ca, caudal vertebrae; cn, ento-, meso-, and ecto-cuneiforms; co, coronoid process of dentary; cp, carpals; cs, calcaneus; ec, ectepicondyle and supinator shelf (humerus); ef, entepicondyle foramen; ep?, probable epipubis; is, ischium; J, jugal; L1-6, lumbar ribs 1 to 6; m, molars; mb, manubrium of malleus; mp, metacarpals; mx, maxilla; px, premaxilla; ra, radius; rc, radial condyle; S1-2, sacrals 1 and 2; sp, extratarsal ("poisonous") spur; t4-t14 (preserved ribs through thoracic 17); uc, ulnar condyle; ul, ulna.

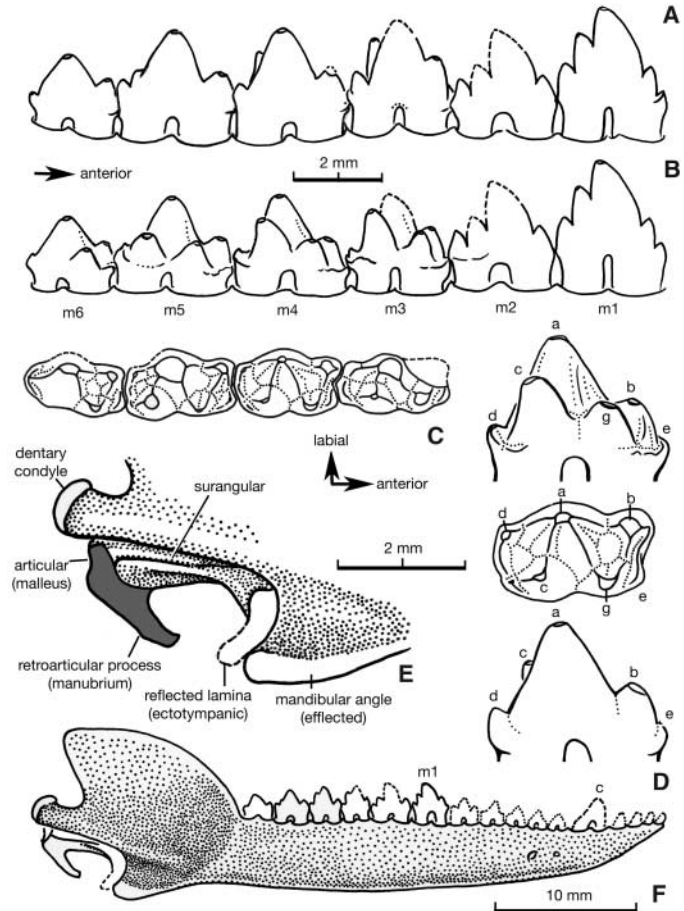


posterior aspect of the mandibular angle accommodates the ectotympenic (angular). The posterior position of the ectotympenic concavity on the mandibular angle in docodontans is different from and more derived than that in the mammaliaforms *Sinoconodon* and *Morganucodon*, in which the ectotympenic concavity is on the medial aspect of the mandibular angle (6, 7). The manubrium of the malleus (retroarticular process of the articular) is anteriorly curved and long in comparison with the short manubrium of *Morganucodon* and *Sinoconodon* (6, 7, 27). The proportion of the malleus manubrium is similar to that of extant monotremes, although slightly more robust than in the latter. *Castorocauda* is similar to crown Mammalia and more derived than *Sinoconodon*, *Morganucodon*, and all pre-mammaliaform cynodonts (27) in preserved middle ear features.

Our analyses, including new characters of *Castorocauda*, corroborate that docodontans are a mammaliaform clade, less derived than *Hadrocodium* but more derived than *Sinoconodon* and *Morganucodon* (1, 8, 26, 28, 29). Among docodontans, *Castorocauda* is closely related to the Middle Jurassic *Krusatodon* and *Simpsonodon* of England (9–11), suggesting interchange between faunas of the Eurasian landmasses during the Middle Jurassic time.

Integument. The fur of *Castorocauda* is preserved as impressions of guard hairs and carbonized under-furs. Hairs and hair-related integument structures are important characteristics of all modern mammals (30, 31). Several younger fossils within the crown Mammalia are preserved with fur, including basal eutherians and metatherians (32, 33), multituberculates,

Fig. 2. Dentition and mandible of *Castorocauda lutrasimilis* (JZMP04-117). **(A)** Labial view of lower molars 1 to 6. **(B)** Lingual view of lower molars 1 to 6. **(C)** Crown view of lower molars 3 to 6. **(D)** Cusp pattern [cusp designation from (11, 12)]. **(E)** Middle ear bones. **(F)** Reconstructed mandible and middle ear bones (lateral view). c, canine; m, molars.



eutricodontans, and symmetrodonts (1). This indicates that the presence of fur is ancestral for the crown Mammalia. *Castorocauda* further shows that fur was also present in mammaliaform relatives of modern mammals (Fig. 3A)

and that the origins of biological adaptations of mammalian integument, such as tactile sensory function and thermal insulation, occurred before the origin of the crown Mammalia (30, 31).

Swimming and fossorial adaptations. Mammals with fossilized pelage from the Early Cretaceous Yixian Formation have few or no hairs on the tail posterior to the pelvic area,

indicating that their tails were naked or scaly. By contrast, *Castorocauda* shows a broad outline of preserved fur on the tail, which is at least 50% wider than the pelvic width along the

length of the tail. Carbonized scales are present adjacent to caudal vertebrae 9 through 20 but are best seen on both sides of caudals 11 through 18 (Fig. 1). The proximal 25% of the tail is covered by guard hairs, the middle 50% mostly covered by scales with sparse hairs, and the distal 25% by scales interspersed with guard hairs. The broad and scaly tail of *Castorocauda* was similar to that of the modern beaver *Castor canadensis*, a semiaquatic placental mammal well adapted for swimming.

Postcranial skeletal features of *Castorocauda* also show specializations for swimming. Caudal vertebrae 5 through 13 have dorsoventrally compressed centra, with the more posterior vertebrae completely flattened. Caudal vertebrae 5 through 15 have bifurcate transverse processes. Both are key features of placental mammals with tails specialized for swimming (34). In caudal vertebrae 5 through 7, the cranial transverse process is much longer than the caudal transverse process. The flattened centrum and bifurcate transverse processes form a distinctive “butterfly” pattern (Fig. 4). This is identical to caudals 9 through 12 of the beaver (Fig. 4). In caudals 7 through 10, the cranial and caudal transverse processes are of approximately equal size and are similar to caudals of the river otter *Lutra canadensis*. In caudals 10 through 18, the transverse processes are reduced and the vertebral outline is graded into an hourglass shape. These vertebral and tail characteristics in this Middle Jurassic docodontan are very similar to those of modern beavers and otters, mammals capable of paddling and/or dorsoventral caudal undulation for propulsion in swimming (34, 35). Remnants of soft tissue between pedal digits suggest some webbing of hind feet.

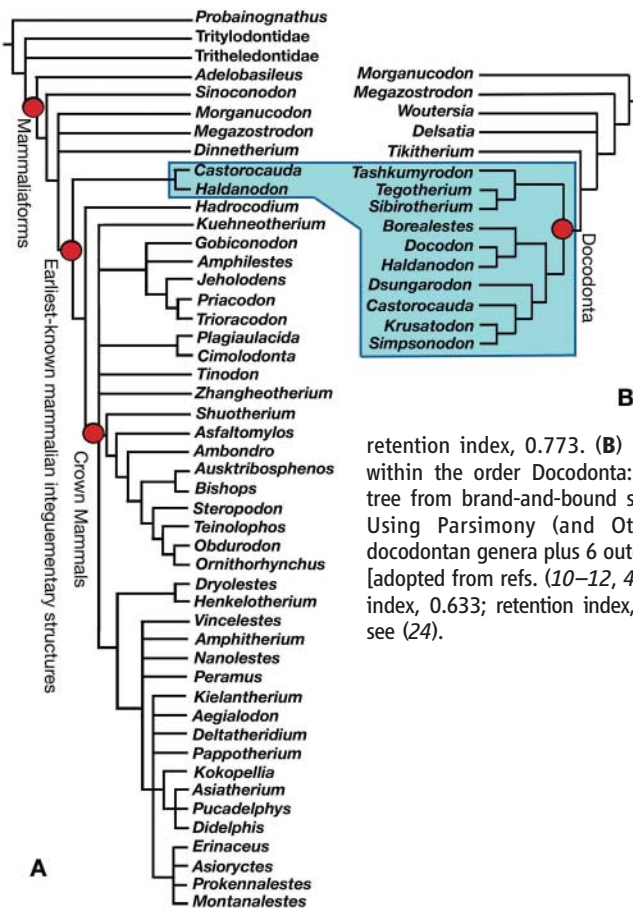
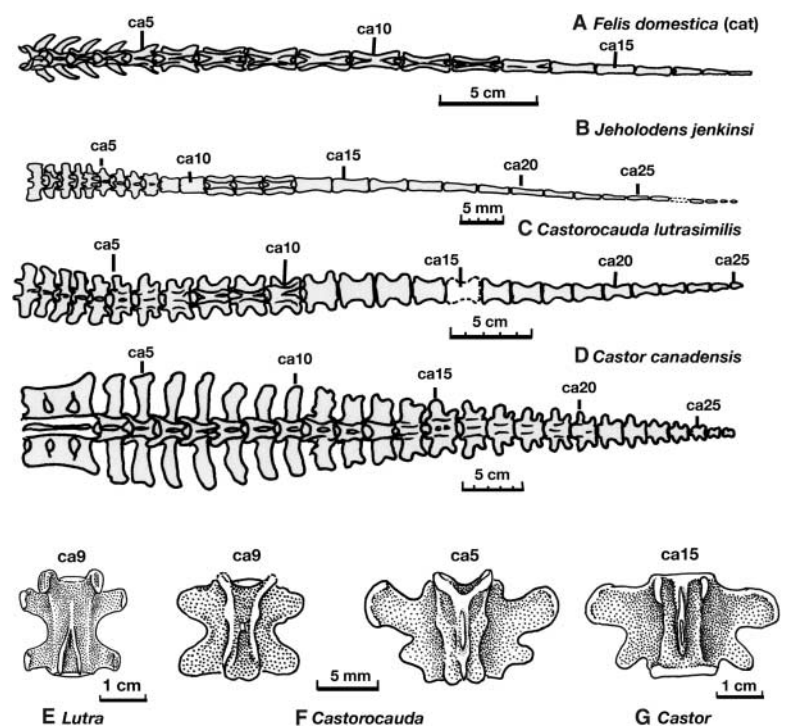


Fig. 3. Phylogenetic relations of the docodontan *Castorocauda lutasimilis*. **(A)** Relation of *Castorocauda* to other mammaliaforms (including crown Mammalia): the strict consensus of 74 equally parsimonious trees from 1000 heuristic runs of PAUP (version 4.0b10) search of a data set of 48 taxa and 281 characters [emended from refs (1, 28, 29, 42, 43)]; for each of the 78 parsimonious trees: tree length, 941; consistency index, 0.507; retention index, 0.773. **(B)** Relationships of *Castorocauda* within the order Docodonta: the single most parsimonious tree from brand-and-bound search of Phylogenetic Analyses Using Parsimony (and Other Methods) 4.0b10 of 9 docodontan genera plus 6 outgroups and 19 dental characters [adopted from refs. (10–12, 43)]; tree length, 49; consistency index, 0.633; retention index, 0.755. For details of analyses, see (24).

Fig. 4. Comparison of the caudal vertebrae of *Castorocauda lutasimilis* and other mammals (A to E scaled to about the same tail length, all dorsal view). **(A)** *Felis domestica* (cat), a generalized terrestrial mammal. **(B)** *Jeholodens jenkinsi* (eutriodontan), a terrestrial mammal of the Early Cretaceous. **(C)** *Castorocauda* (JZMP04117), all caudal vertebrae. **(D)** *Castor canadensis* (modern beaver), all caudal vertebrae. **(E)** *Lutra canadensis* (river otter), caudal 9. **(F)** *Castorocauda*, caudals 5 and 9. **(G)** Beaver, caudal 15. Transverse processes are present in proximal caudal vertebrae of all mammals but are reduced markedly in the vertebrae posterior to the pelvis and are absent in more distal caudal vertebrae of generalized terrestrial mammals (e.g., *Felis* and *Jeholodens*). In semiaquatic placentals, the hypertrophied and bifurcate transverse processes form a “butterfly” or “horizontal H” pattern in caudal vertebrae that are correlated with the scaly and paddlelike tail of the beaver (34). The Middle Jurassic *Castorocauda* developed similar caudal vertebral structures and had a broad, flattened, scaly tail as in modern beavers. Its semiaquatic feeding adaptation is similar to that of the modern river otter.



Both *Castorocauda* and the Late Jurassic docodontan *Haldanodon* are similar to the modern monotreme *Ornithorhynchus* in forelimb fossorial specializations (28–36). The distal humerus is wide; it has hypertrophied epicondyles, a supinator process, and massive and widely separated ulnar and radial condyles. The ulna has a massive and asymmetrical olecranon process. The radius is robust. The carpals are blocklike, and the metacarpals and proximal phalanges are robust and wide. A single and large sesamoid bone for the digital flexor muscle tendon is present at the metacarpal-phalangeal joint.

The forelimb of *Ornithorhynchus* is adapted to digging and also used for rowing during swimming and diving (35–37). It has been hypothesized that the docodontan *Haldanodon* was semiaquatic (28, 38). From the additional evidence of *Castorocauda*, it appears that many docodontans were burrowing mammals with sprawling limb posture and gait in terrestrial locomotion. They may have also used the forelimbs for rowing during swimming, as an exaptation (37), as in the platypus.

Plated ribs. Based on the preserved ribs and vertebral bodies, we estimate that *Castorocauda* probably had 14 thoracic, 7 lumbar, 3 sacral and 25 caudal vertebrae (Fig. 1). The proximal portions of the thoracolumbar ribs have broad costal plates; the adjacent costal plates overlap by at least one-third of the plate width. The costal plates resemble the plated thoracolumbar ribs of the cynodonts *Thrinaxodon*, *Cynognathus* (39), and *Diademodon* (40), although *Castorocauda* differs in lacking the costal tubercles (ridges) and in the absence of interlocking of adjacent costal plates seen in *Cynognathus* and *Diademodon* (39). Among Mesozoic mammals, the gobiconodontid *Repenomamus* has costal plates in the anterior lumbar and posterior thoracic ribs, but these are far less developed than those in *Castorocauda*.

Plated ribs have a homoplastic distribution among cynodonts and mammaliaforms. They are absent in the traversodontids but present in the closely related diademodontids. Costal plates are absent in many intermediate groups between primitive cynodonts *Diademodon*, *Cynognathus*, and *Thrinaxodon*, and the more derived *Castorocauda*. It is parsimonious to hypothesize that *Castorocauda* represents a reversal (or convergence) to cynodonts in the development of costal plates. Plated lumbar ribs probably increase the insertion area for the M. iliocostalis muscle and reinforce the support of the adjacent vertebral segments by interlocking adjacent ribs, thereby strengthening the trunk (39). Thoracolumbar rib plates are present (although much narrower) in xenarthran mammals with either fossorial or arboreal adaptations (39). The plated ribs of *Castorocauda* are very thin and lack the pachyosteosclerosis (hypertrophied growth of the highly compact

bones for buoyancy control), a characteristic of fully aquatic and much larger sirenian mammals.

Castorocauda is the largest known Jurassic mammaliaform (including mammals). By its preserved skull length of ≥ 60 mm and the well-established scaling relation of skull and body mass (8, 41), we estimate that the body mass of the holotype specimen was at least 500 g. The preserved length from rostrum to tail is 425 mm, but the actual body length is certainly greater. The length of female platypuses with similar fossorial and semiaquatic habits ranges from 390 to 550 mm, corresponding to a body mass range of 700 to 2400 g. We estimate the upper limit of body mass to be approximately 800 g for *Castorocauda*. All other Jurassic mammals are small (7). Constrained by their small size, most were generalized terrestrial insectivores or omnivores. Previously, the largest taxon was *Sinoconodon rigneyi* (7); its largest individuals reached an estimated body mass of 500 g (8). Based on its relatively large size, swimming body structure, and anterior molars specialized for piscivorous feeding, *Castorocauda* was a semiaquatic carnivore, similar to the modern river otter. This fossil shows that basal mammals occupied more diverse niches than just those of small insectivorous or omnivorous mammals with generalized terrestrial locomotory features. *Castorocauda* also suggests that mammaliaforms developed physiological adaptations associated with pelage, well before the rise of modern Mammalia, and had more diverse ecomorphological adaptations than previously thought, with at least some lineages occupying semiaquatic niches.

References and Notes

- Z. Kielan-Jaworowska, R. L. Cifelli, Z.-X. Luo, *Mammals from the Age of Dinosaurs: Origins, Evolution and Structure* (Columbia Univ. Press, New York, 2004).
- D. Sigogneau-Russell, *Comp. Rend. de l'Acad. des Sci. Paris* **327**, 571 (1998).
- J. J. Flynn, J. M. Parrish, B. Rakotosamimanana, W. F. Simpson, A. E. Wyss, *Nature* **401**, 57 (1999).
- P. M. Butler, W. A. Clemens, *Palaeontology* **44**, 1 (2001).
- T. Martin, O. W. M. Rauhut, *J. Vertebr. Paleontol.* **25**, 414 (2005).
- K. A. Kermack, F. Mussett, H. W. Rigney, *Zool. J. Linn. Soc.* **53**, 87 (1973).
- A. W. Crompton, Z.-X. Luo, in *Mammal Phylogeny: Mesozoic Differentiation, Multituberculates, Monotremes, Early Therians, and Marsupials*, F. S. Szalay, M. J. Novacek, M. C. McKenna, Eds. (Springer-Verlag, New York, 1993), pp. 30–44.
- Z.-X. Luo, A. W. Crompton, A.-L. Sun, *Science* **292**, 1535 (2001).
- K. A. Kermack, A. J. Lee, P. M. Lees, F. Mussett, *Zool. J. Linn. Soc.* **89**, 1 (1987).
- D. Sigogneau-Russell, *Acta Palaeontol. Pol.* **48**, 357 (2003).
- T. Martin, A. O. Averianov, *J. Vertebr. Paleontol.* **24**, 195 (2004).
- P. M. Butler, *J. Vertebr. Paleontol.* **17**, 435 (1997).
- A. O. Averianov et al., *Acta Palaeontol. Pol.* **50**, 789 (2005).
- Etymology: *Castor* (Latin), beaver; *cauda* (Latin), tail; after the broad, flattened, scaly, and beaverlike tail for swimming; *lutra* (Latin), otter; *similis* (Latin), similar; similar to extant otters in some dental and vertebral characters. Systematics: Clade Mammaliaformes (Class Mammalia by traditional definition); Order Docodonta; Family *incertae sedis*; gen. et sp. nov. *Castorocauda lutrasimilis*. Holotype: Jinzhou Museum of Paleontology, Jinzhou City, Liaoning Province, China (JZMP-04-117), an incomplete, flattened skeleton, partial skull, preserved with fur and scales. Locality and Age: Daohugou locality (N41°18.979', E119°14.318'), Ningcheng County, Inner Mongolia, China; Jiulongshan Formation, dated to be 164 million years ago (15–17).
- W. Chen, Q. Ji, D.-Y. Liu et al., *Geol. Bull. China* **23**, 1165 (in Chinese) (2004).
- Y.-Q. Liu, Y.-X. Liu, *Geophys. Res. Lett.* **32**, L12314 (2005).
- Q. Ji et al., *Mesozoic Jehol Biota of Western Liaoning, China* (Geol. Publ. House, Beijing, 2004).
- X.-L. Wang, Z.-H. Zhou, F.-C. Zhang, X. Xu, *Chin. Sci. Bull.* **47**, 226 (2002).
- X. Xu, F.-C. Zhang, *Naturwissenschaften* **92**, 173 (2004).
- K.-Q. Gao, N. Shubin, *Nature* **422**, 424 (2003).
- D. Ren et al., *Geol. Bull. China* **21**, 584 (2002) (in Chinese).
- Y. Shen, P. Chen, D. Huang, *J. Stratigraphy* **27**, 311 (2003) (in Chinese).
- Diagnosis: Lower dentition i4, c1, p5, m6 (Fig. 2). *Castorocauda lutrasimilis* has the typical docodontan molar features in molars 3 to 6 but is distinguishable from other docodontans by the mediolaterally compressed molars 1 and 2 with slightly recurved cusps in alignment. In mandibular length, *C. lutrasimilis* is about twice as large as *Docodon*, the next largest docodontan. See also (24).
- Materials and methods are available as supporting material on Science Online.
- M. A. O'Leary, in *The Emergence of Whales*, J. G. M. Thewissen, Ed. (Plenum Press, New York, 1998), pp. 133–161.
- J. A. Lillegraven, G. Krusat, *Contrib. Geol. Univ. Wyoming* **28**, 39 (1991).
- E. F. Allin, J. A. Hopson, in *The Evolutionary Biology of Hearing*, D. B. Webster, R. R. Fay, A. N. Popper, Eds. (Springer-Verlag, New York, 1992), pp. 587–614.
- T. Martin, *Zool. J. Linn. Soc.* **145**, 219 (2005).
- Z.-X. Luo, Z. Kielan-Jaworowska, R. L. Cifelli, *Acta Palaeontol. Pol.* **47**, 1 (2002).
- L. Alibardi, P. F. A. Maderson, *J. Morphol.* **258**, 49 (2003).
- T. S. Kemp, *The Origin and Evolution of Mammals* (Oxford Univ. Press, Oxford, 2005).
- Q. Ji et al., *Nature* **416**, 816 (2002).
- Z.-X. Luo, Q. Ji, J. R. Wible, C.-X. Yuan, *Science* **302**, 1934 (2003).
- N. Rybczynski, W. McLellan, *J. Vertebr. Paleontol.* **25**, 107A (2005).
- J. G. M. Thewissen, F. E. Fish, *Paleobiology* **23**, 482 (1997).
- P. P. Gambaryan, A. A. Aristov, J. M. Dixon, G. Y. Zubtsova, *Russ. J. Theriology* **1**, 1 (2002).
- F. E. Fish, P. B. Frappell, R. V. Baudinette, P. M. MacFarlane, *J. Exp. Biol.* **204**, 797 (2001).
- T. Martin, M. Nowotny, in *Guimarota: A Jurassic Ecosystem*, T. Martin, B. Krebs, Eds. (Pfeil, Munich, 2000), pp. 91–96.
- F. A. Jenkins Jr., *Peabody Mus. Nat. His. Bull.* **36**, 1 (1971).
- A. S. Brink, *Palaeontol. Afr.* **3**, 3 (1955).
- P. D. Gingerich, B. H. Smith, in *Size and Scaling in Primate Biology*, W. L. Jungers, Ed. (Plenum, New York, 1984), pp. 257–272.
- Z.-X. Luo, R. L. Cifelli, Z. Kielan-Jaworowska, *Nature* **409**, 53 (2001).
- H.-U. Pfretzschner, T. Martin, M. Maisch, A. Matze, G. Sun, *Acta Palaeontol. Pol.* **50**, 799 (2005).
- We thank Z.-Y. Sun and the Jinzhou Museum of Paleontology for making this specimen available for us to study. We also thank K. C. Beard, M. R. Dawson, T. Martin, N. Rybczynski, and J. R. Wible for numerous discussions; M. R. Dawson for improving the manuscript; M. A. Klingler for assistance with graphics; J. R. Wible for

Supporting Online Material

www.sciencemag.org/cgi/content/full/311/5764/1123/DC1
SOM Text

28 November 2005; accepted 23 January 2006
10.1126/science.1123026

REPORTS

X-ray Flares from Postmerger Millisecond Pulsars

Z. G. Dai,^{1*} X. Y. Wang,¹ X. F. Wu,² B. Zhang³

Recent observations support the suggestion that short-duration gamma-ray bursts are produced by compact star mergers. The x-ray flares discovered in two short gamma-ray bursts last much longer than the previously proposed postmerger energy-release time scales. Here, we show that they can be produced by differentially rotating, millisecond pulsars after the mergers of binary neutron stars. The differential rotation leads to windup of interior poloidal magnetic fields and the resulting toroidal fields are strong enough to float up and break through the stellar surface. Magnetic reconnection–driven explosive events then occur, leading to multiple x-ray flares minutes after the original gamma-ray burst.

Gamma-ray bursts (GRBs) are flashes of gamma rays occurring at the cosmological distances. They fall into two classes (1): short-duration (<2 s) hard-spectrum bursts and long-duration soft-spectrum bursts. Long GRBs result from core collapses of massive stars (2), and short GRBs appear to be produced in mergers of neutron star binaries or black hole–neutron star binaries (3–9). Recently, thanks to accurate localizations of several short GRBs (3, 6, 8) by satellites Swift and High Energy Transient Explorer 2 (HETE-2), the multiwavelength afterglows from these events have been detected and the associated host galaxies have been identified. The observations provide a few pieces of evidence in favor of the binary compact object merger origin of short GRBs (10–12). Because it takes ~0.1 to 1 billion years of gravitational wave radiation before the binary coalesces, at least some short GRB host galaxies should contain a relatively old stellar population. Because neutron stars in the binary system usually receive a very high natal velocity, the merger site is preferably at the outskirts of the host galaxy, and the circumburst medium density is likely low. These characteristics have been revealed by recent observations: First, the

identified elliptical galaxies associated with GRB 050509B (3, 4) and GRB 050724 (8, 9) suggest that these hosts are early-type galaxies with a low star-formation rate, ruling out progenitor models invoking active star formation. Second, the nondetection of any supernova signal from GRB 050709 indicates that short bursts are not associated with collapses of massive stars (5, 7). Third, afterglow modeling of GRB 050709 suggests a low-density environment (13), which is consistent with that of the outskirts of the host galaxy or that of an intergalactic medium.

However, the above merger origin was recently challenged by the discovery of x-ray flares occurring after two short bursts. X-ray flares were discovered to occur at least ~100 s after the triggers of the short GRB 050709 (5) and GRB 050724 (8). These flares require that the central engine is in long-lasting activity. This requirement conflicts with the current models involving neutron star–neutron star mergers (14, 15) or neutron star–black hole mergers (16), because all of these models are attached to a common postmerger picture that invokes a black hole surrounded by a torus. The predicted typical time scales for energy release are much shorter than ≥100 s, as observed in GRBs 050709 and 050724. Therefore, understanding the origin of x-ray flares from short bursts is currently of great interest. Here, we show that such flares can be produced by differentially rotating, millisecond pulsars with typical surface magnetic fields that occur after the mergers of binary neutron stars.

In the conventional scenarios of short bursts (10–12), after the merger of a neutron

star binary, a stellar-mass black hole is formed with a transient torus of mass ~1 to 10% of the total. These scenarios are valid if the total mass (~2.5 to 2.8 M_{\odot} , where M_{\odot} is the solar mass) of the postmerger object is larger than the maximum mass of a nonrotating Tolman–Oppenheimer–Volkoff neutron star, $M_{\max,0}$. This is valid if the nuclear equation of state (EOS) is soft to moderately stiff (17). However, the total mass of the postmerger object is smaller than $M_{\max,0}$ for very stiff EOSs on the basis of mean field theory (17). Timing observations of the millisecond pulsar J0751+1807 in a circular binary system with a helium white-dwarf companion (18) reveal the existence of a neutron star with mass of $2.1 \pm 0.2 M_{\odot}$ (at the 1 σ confidence level). This measurement implies that the maximum mass of nonrotating neutron stars must be larger than $2.1 M_{\odot}$ so that stiff EOSs are favored. Furthermore, recent general relativistic numerical simulations (17, 19) have shown that for stiff to very stiff nuclear EOSs, the postmerger object is indeed a differentially rotating massive neutron star with period of ~1 ms, because uniform rotation and differential rotation can support a maximum mass ~20 and ~50% higher than $M_{\max,0}$, respectively. It is therefore reasonable to assume the existence of a differentially rotating millisecond pulsar after a double neutron star merger. Such a pulsar should also be surrounded by a hot torus with mass ~0.01 to 0.1 M_{\odot} . Similar to the previous scenarios, a short burst may be produced by the Parker instability in the torus (11) or the annihilation of neutrinos emitted from the torus (12).

After the GRB trigger, differential rotation starts to wind the interior magnetic field into a toroidal field (20, 21). To represent physical processes of windup and floating of the magnetic field, we considered a simple two-component model in which the star is divided into two zones with a boundary at the radius $R_c \cong 0.5 R_*$ (where R_* is the stellar radius): the core and the shell components. Their moments of inertia are I_c and I_s and their angular (rotation) velocities are Ω_c and Ω_s , respectively. The differential angular velocity is then $\Delta\Omega = \Omega_c - \Omega_s$ and its initial value (marked by a subscript zero) is taken as $(\Delta\Omega)_0 = A_0\Omega_{s,0}$ (where A_0 is the ratio of the initial differential angular velocity to the shell's initial angular velocity). If the radial magnetic field compo-

¹Department of Astronomy, Nanjing University, Nanjing 210093, China. ²Purple Mountain Observatory and Joint Center for Particle Nuclear Physics and Cosmology of Purple Mountain Observatory–Nanjing University, Chinese Academy of Sciences, Nanjing 210008, China. ³Department of Physics, University of Nevada, Las Vegas, NV 89154, USA.

*To whom correspondence should be addressed. E-mail: dzg@nju.edu.cn